ISSN: 0067-2904

A Novel Total Variation Model for Image Denoising with Different Types of Noise

Ahmed K. Al. Ajberi*, Zahra R. Jawad
Department of Mathematics, College of Education for Pure Science, University of Basrah, Basrah, Iraq

Received: 24/4/2024 Accepted: 17/8/2024 Published: 30/9/2025

Abstract

Image denoising is a computer vision task that mainly aims to remove unwanted noise from a given image while preserving all necessary details and related information. Detection of edges and smooth image generation are required criteria for measuring the quality of the image denoiser. This paper introduces a new model for image denoising based on total variation (TV). The unprecedented novelty total variation (NTV) model combines $\ell_1$norm-based total variation (TV) and ℓ_2 norm-based TV regularization. This paper uses the implicit finite difference method to solve the NTV model numerically. The statistical measurements are used to compare the results obtained using the NTV model with those obtained using other models, which show the superiority of the proposed model in terms of its effectiveness and efficiency through removing different types of noise from images. This proposed model is effective in detail sharpening and texture preservation.

Keywords: Image Denoising, Regularization Technique, Total Variation, Anisotropic Technique, Isotropic Technique, Implicit Finite Difference Method.

نموذج جديد للتباين الكلي لتقليل ضوضاء الصور بأنواع مختلفة من الضوضاء

احمد كاظم الجابري, زهراء رعد جواد

قسم الرياضيات, كلية التربية للعلوم الصرفة, جامعة البصرة, البصرة, العراق

الخلاصة

تقليل ضوضاء الصورة هي مهمة رؤية حاسوبية تهدف بشكل أساسي إلى إزالة الضوضاء الغير مرغوبه من صورة معينة مع الحفاظ على جميع التفاصيل الضرورية والمعلومات ذات الصلة. ستعمل عملية تقليل الضوضاء على إزالة كل هذه الأنواع من الضوضاء. يعد الكشف عن الحواف وتنعيم الصورة هو من المعايير المطلوبة لقياس جودة معالج ضوضاء الصور. تقدم هذه الورقة نموذج جديد لإزالة الضوضاء القائم على التباين الكلي (TV). يتم تقديم نموذج التباين الكلي الجديد (NTV) يجمع بين معيار ℓ_1 القائم على تنظيم التباين الكلي (TV) ومعيار ℓ_2 القائم على تنظيم التباين الكلي. يستخدم هذا البحث طريقة الفروقات المنتهية الضمنية لحل النموذج (NTV) عدديا. تم استخدام القياسات الإحصائية لمقارنة النتائج التي تم الحصول عليها باستخدام نموذج NTV مع تلك التي تم الحصول عليها باستخدام النماذج الأخرى، حيث تبين تفوق

* Email: ahmed.shanan@uobasrah.edu.iq

النموذج المقترح من حيث فعاليته وكفاءته من خلال إزالة أنواع ضوضاء مختلفة من الصور. النموذج المقترح فعال في تعزيز التفاصيل والحفاظ على الملمس.

1. Introduction

Over the last two decades, an increased interest in and use of mathematical models has been observed in different domains, such as engineering, physics, computer science, and so on. These mathematical models have been used in computer science applications such as denoising, inpainting, segmentation, zooming, and super-resolution for images [1]. Generally, many types of noise will be included in images obtained from acquisition and compression, making certain areas of the image too difficult to interpret. Low-quality cameras and poor light may also add some noise to the image. Techniques based on regularization variational and partial differential equations (PDEs) have been used and investigated in these domains recently due to their modeling flexibility and numerical application advantages [2].

In this paper, the use of PDEs in the noise reduction problem in digital images will be studied because it is still an active research field that arouses researchers' interest in image processing. Image noise results from several reasons, such as sensor defects [3], transmission problems [4], natural noise [5], image compression [6], etc. There are several techniques introduced for noise removal in images, such as Variational [1], [7], Spatial domain filtering [8], Transform domain filtering [9], Low-rank denoising [10], Sparse representation [11], and Deep learning-based denoising [12]. Various challenges remain unresolved in removing noise from images when using different types of noise.

PDE-based image denoising methods are a tool for image smoothing. As a result, one of the primary considerations when selecting a technique for creating image noise reduction models is how well it preserves the image's characteristics during smoothing [13]. The methods based on a TV concept will be particularly studied. The criterion of TV is high efficiency in various other image processing tasks. One explanation for this is that the TV operator enforces a concept of regularity that is well-suited to images: it penalizes oscillations and random fluctuations while allowing discontinuities. This is an intriguing trait because genuine images typically have discontinuities in the intensity map generated by occluding elements in the scene.

In 1992, Rudin, Osher, and Fatemi (ROF) initially proposed the use of Total Variation (TV) for image-denoising [14]. The ROF approach is introduced based on TV minimization for noise removal in images, where it often produces denoised images with odd local configurations that allow for a minimal overall TV. This is known as the gradient effect [15]. TV operators find application in denoising and broader signal restoration issues such as compressed sensing [16], deconvolution [17], interpolation [18], colorizing [19], and inpainting [20]. Furthermore, the concept of TV was developed and expanded in various ways [21]. Yang, Bo, et al. investigated the suitability of the TV denoising technique for preprocessing NPP signals [22]. Afonso, Manya V. et. al used the TV regularization method to study image reconstruction with missing pixels or noise-corrupted images [23].

M. Grasmair and F. Lenzen suggested a combination and addition of anisotropy to the TV regularization to improve the result and treatment of the gradient that the TV suffers from [24]. C. Qiang et al. created a mathematical model based on TV based on a new edge index called difference curvature that can distinguish between scarps and slopes [25].

G. Lin et al. put up a three-dimensional model for the problem of deblurring 3D images, based on fractional total variation (3DFTV) [26]. P. Cong Thang et al. introduced a novel model in which the regularization term combined TV and high-order TV. Additionally, the authors investigated the existence and uniqueness of the minimizer for the model under consideration. The results of the experiments are given to show how effective the suggested model is [27].

This paper proposes a new combining denoising model to deal with different types of noise in images. The model was built based on combining TV-ℓ_1, and TV-ℓ_2, enabling the denoising method to remove the noise and preserve the edges and corners in the images without artifacts; more details can be found in Section 3. The rest of the paper is organized as follows: Linear and non-linear TV denoising models are presented in Section 2. The proposed TV denoising model is introduced in Section 3. Several numerical results of the proposed model and other models for image noise reduction have been presented and compared, and the conclusions will be discussed and presented in Section 4. Finally, the conclusions are introduced in Section 5.

2. Image denoising based on linear and nonlinear TV Models

Let an image u defined as $u : \Omega \rightarrow R$, and $M \times N$ represented by the size of u, and Ω is the image domain. The derivatives $\partial_x u, \partial_y u$ of u in x and y directions respectively were defined as below:

$$\partial_x u_{i,j} = \begin{cases} u_{i,j} - u_{i-1,j} & 1 < i \leq M, \quad 1 \leq j \leq N \\ u_{i,j} - u_{M,j} & i = 1, \quad 1 \leq j \leq N \end{cases} \tag{1}$$

$$\partial_y u_{i,j} = \begin{cases} u_{i,j} - u_{i,j-1} & 1 \leq i \leq M, \quad 1 < j \leq N \\ u_{i,j} - u_{i,N} & 1 \leq i \leq M, \quad j = 1 \end{cases} \tag{2}$$

Where x is the horizontal direction, and y is the vertical direction of u. Then the gradient was defined as follows:

$$\nabla u = (\partial_x u, \partial_y u)^{\top}, \tag{3}$$

The nonlinear model of TV-ℓ_1 was introduced by Rudin et al. in 1992 [14]. It is formulated by:

$$\min_u \frac{\lambda}{2} \| f - u \|_2^2 + \| \nabla u \|_{\ell_1}, \tag{4}$$

where f is a noised image, $\lambda > 0$ is a parameter that controls the trade-off between data fidelity and regularization, and u is the desired image. The minimization of functional (4) has been solved by Euler Lagrange equation. Then, the gradient descent method has been applied to it:

$$u_t = \lambda(f - u) + \nabla \cdot \frac{\nabla u}{|\nabla u|} \tag{5}$$

Where t represents the time, and u_t represents the change of u in the time direction. Smaller λ is useful for eliminating noise, whilst larger λ aids in maintaining image features. The image gradient in the TV-ℓ_1 model was used to regularize images and performed well in preserving edges during noise removal. It is frequently utilized in several image problems, even though it can produce a staircase effect through processing, (for details, see [28]).
While the linear model of TV-ℓ_2 was also proposed in 1992 by Rudin et al. [14], the formula for this model is introduced as follows:

$$\min_u \lambda\|f - u\| + \|\nabla u\|_{\ell_2}, \quad (6)$$

The minimization of functional (6) has been solved by Euler Lagrange equation, then the gradient descent method has been applied to it:

$$u_t = \lambda(f - u) + \Delta u \quad (7)$$

Where t represents the time, and u_t represents the change of u in the time direction. The image gradient in TV-ℓ_2 model was applied to regularize images and performed poorly in preserving edges during noise removal. Furthermore, the connectivity principle is not satisfied, and the curvature preservation is not maintained when using this model to remove noise in images. The information is propagated in all directions by applying this model, which results in blurry images and the loss of edges.

3. Proposed Total Variation Model

To address the defect of obtaining a blurry image during noise removal and edge loss using TV-ℓ_1 and TV-ℓ_2 models. This paper introduced a novel total variation model (NTV) for noise removal in the images. This model is introduced based on combining TV-ℓ_1 and TV-ℓ_2 models as below:

$$\min_u \lambda\|f - u\| + \alpha\|\nabla u\|_{\ell_1} + \beta\|\nabla u\|_{\ell_2} \quad (8)$$

Where the value of β parameter is used to control noise removal in low-texture images, while the α is applied to control the texture reconstruction in high-texture images. The minimization of functional (8) has been solved by Euler Lagrange equation, and then the gradient descent method has been applied to it:

$$u_t = \lambda(f - u) + \alpha\nabla \cdot \frac{\nabla u}{|\nabla u|} + \beta\Delta u \quad (9)$$

Where t represents the time, and u_t represents the change of u in the time direction. In this model, the values of β, α, and λ parameters are used to control noise removal and reconstruct the edges and corners in the images. These parameters will help to control dealing with different values of texture images. This proposed model is introduced to face the drawbacks of TV-ℓ_1 and TV-ℓ_2 models, its results overcome those obtained using TV-ℓ_1 and TV-ℓ_2 models.

4. Numerical Experiments

In the field of numerical methods, many articles have used these methods to solve equations numerically [29], [30], [31]. In this paper, TV-ℓ_1, TV-ℓ_2 and NTV models are numerically solved using the implicit finite difference method (IFDM) to evaluate their performance. The IFDM is applied to solve TV-ℓ_1 in (5) TV-ℓ_2 in (7) and NTV in (9), separately. The noise removal procedure was implemented in MATLAB code, where (elapsed for MATLAB, version R2023a). Natural images in the Berkeley Database [32] are used in these experiments, where they represent the low- and high-texture color images, as seen in Figure 1.

Figure 1: Example of eight out of 100 training natural images.

Figure 2 shows the results of removing the noise from the natural images using TV-ℓ_1 and TV-ℓ_2, and NTV models.

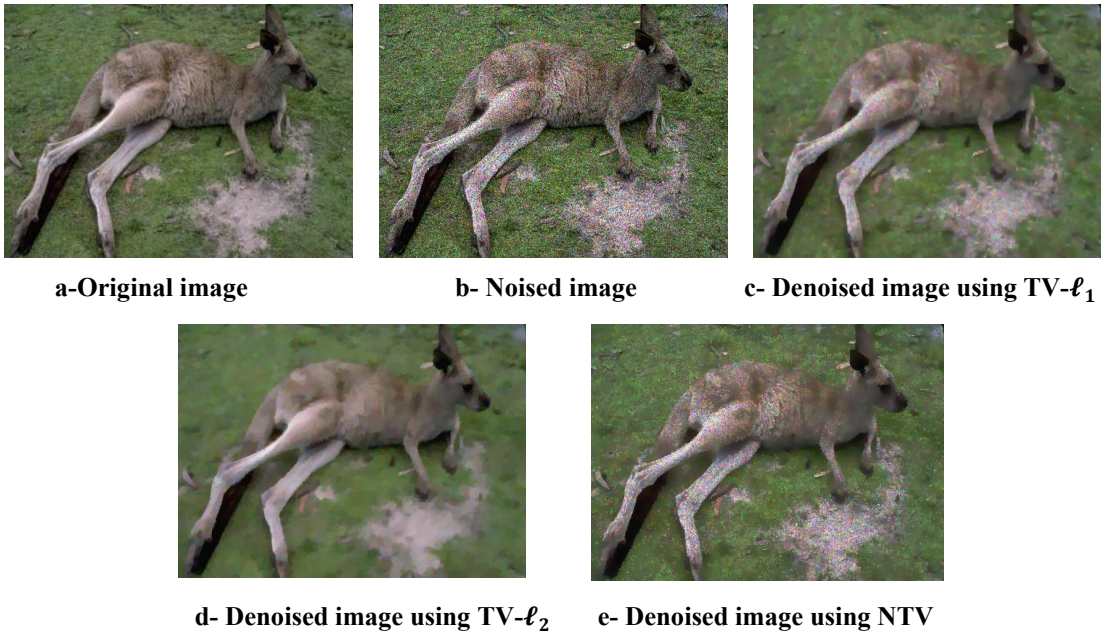

Figure 2: Example of Gaussian noise removal using TV models at 800 iterations.

In Figure 2, it is observed that the denoised image using the NTV model is almost the same as the original image, while the denoised images using TV-ℓ_1 and TV-ℓ_2 models are not the same as the original image. To further check the quality of a denoised image, statistical measurements are used, in particular, to check the efficacy of TV models.
Different types of experiments have been done to study the efficacy and efficiency of the proposed mathematical model for noise removal in the images. In these experiments, the quality of denoised images is checked through comparison with original noise images, using several statistical quality measures (SQMS), such as mean square error (MSE), peak signal-to-noise ratio (PSNR) [33], structural similarity (SSIM) [34], and entropy - of original (Eo), - of denoised (Ed) images [35].

4.1. Different types of noise

The proposed model has been used to remove different types of standard ratio noise in images, such as Gaussian, Speckle, Poisson, and Salt & Pepper [36]. In this experiment, the values of parameters α, and β are used as 0.001, and the iteration is 1000. This experiment is conducted on 100 color images, and the results of the NTV model are contrasted with those obtained using TV-ℓ_1, and TV-ℓ_2. Figure 3 gives different types of standard ratio noise in color images.

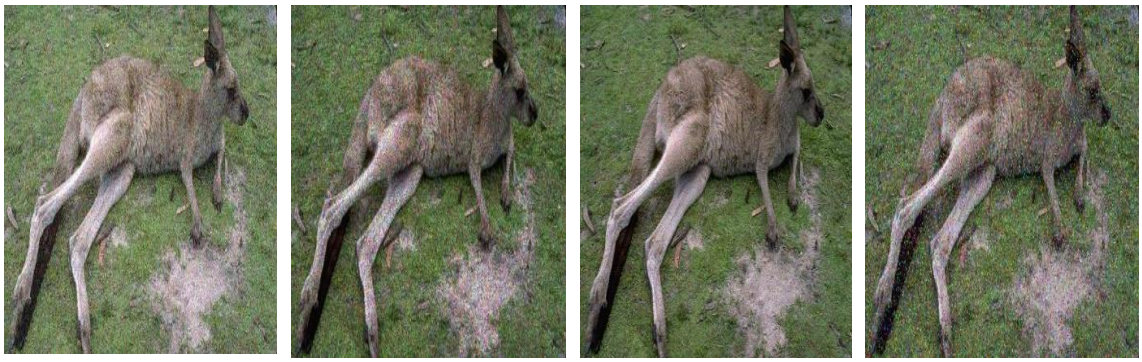

a- Gaussian noise **b- Speckle noise** **c- Poisson noise** **d- Salt & Pepper noise**

Figure 3: Different types of standard ratio noise in color images.

Tables 1–4 summarize the average values of MSE, PSNR, SSIM, entropy, and the time taken to obtain results utilizing these models.

Table 1: Statistical Quality measurements for Gaussian noise removal in images, obtained results using TV-ℓ_1, TV-ℓ_2, and NTV models.

SQMs	MSE	PSNR	SSIM	Eo	Ed	Time (s)
TV-ℓ_1	62.96939	30.33977	0.50031	7.14413	6.77245	29.26082
TV-ℓ_2	49.95006	31.41951	0.56405	7.14413	6.89734	13.77505
NTV	36.51081	32.85549	0.73667	7.14413	6.99208	19.51194

Table 2: Statistical Quality measurements for Speckle noise removal in images, obtained results using TV-ℓ_1, TV-ℓ_2, and NTV models.

SQMs	MSE	PSNR	SSIM	Eo	Ed	Time (s)
TV-ℓ_1	67.34984	30.05256	0.50396	7.14413	6.77181	22.48796
TV-ℓ_2	56.54304	30.85985	0.56369	7.14413	6.87485	18.11611
NTV	45.73279	31.88311	0.70418	7.14413	7.01277	23.04775

Table 3: Statistical Quality measurements for Poisson noise removal in images, obtained results using TV-ℓ_1, TV-ℓ_2, and NTV models.

SQMs	MSE	PSNR	SSIM	Eo	Ed	Time (s)
TV-ℓ_1	63.30611	30.29901	0.50602	7.14413	6.79922	28.12821
TV-ℓ_2	50.48122	31.38211	0.57105	7.14413	6.85615	21.47309
NTV	34.79938	33.09532	0.74005	7.14413	6.94308	25.53961

Table 4: Statistical Quality measurements for Salt & Pepper noise removal in images, obtained results using TV-ℓ_1, TV-ℓ_2, and NTV models.

SQMs	MSE	PSNR	SSIM	Eo	Ed	Time (s)
TV-ℓ_1	61.7071	30.46544	0.49712	7.14413	6.74956	22.79845
TV-ℓ_2	47.9755	31.62312	0.57182	7.14413	6.85447	14.27302
NTV	35.4588	32.94485	0.41603	7.14413	6.93746	16.78843

Tables 1-4 showed the results using the NTV model outperformed those obtained using TV-ℓ_1, and TV-ℓ_2 in terms of noise removal and keeping edges for all these different kinds of noise. Moreover, the above tables indicate that the NTV model is better at removing noise, it yields a higher PSNR with less MSE and gives an SSIM value closer to one. The NTV model also has an entropy closer to the original image entropy than the TV-ℓ_1, and TV-$\ell_2$models.

4.2. Different ratios of added noise

In this experiment, the different ratios of added Salt &Pepper noise to images have been studied to check the performance of the proposed model. The ratios of Salt &Pepper noise are 0.1, 0.2, 0.3, and 0.4 which are applied in this experiment, the iteration is 1000, and the α and β are 0.5. This experiment is conducted on 100 color images, and the results of the NTV model are contrasted with those obtained using TV-ℓ_1, and TV-ℓ_2 models. Figure 4 gives different ratios of added Salt &Pepper noise to color images. Figure 5 gives different ratios of added Gaussian noise to color images.

a- A ratio is 0.1 **b- A ratio is 0.2** **c- A ratio is 0.3** **d- A ratio is 0.4**

Figure 4: Different ratios of added Salt &Pepper noise to color images.

a- A ratio is 0.1 **b- A ratio is 0.2** **c- A ratio is 0.3** **d- A ratio is 0.4**

Figure 5: Different ratios of added Gaussian noise to color images.

Tables 5–8 summarize the average values of MSE, PSNR, SSIM, entropy, and the time taken to obtain results utilizing these models.

Table 5: Statistical quality measurements for Salt & Pepper noise removal in images, noise ratio = 0.1, obtained results using TV-ℓ_1, TV-ℓ_2, and NTV models.

SQMs	MSE	PSNR	SSIM	Eo	Ed	Time (s)
TV-ℓ_1	15.4133	36.31721	0.23876	7.14413	7.03763	0.57254
TV-ℓ_2	13.1203	37.00402	0.23884	7.14413	7.02166	0.83402
NTV	12.3707	37.25565	0.23872	7.14413	6.98050	1.13303

Table 6: Statistical quality measurements for Salt & Pepper noise removal in images, noise ratio = 0.2, obtained results using TV-ℓ_1, TV-ℓ_2, and NTV models.

SQMs	MSE	PSNR	SSIM	Eo	Ed	Time (s)
TV-ℓ_1	27.0363	33.87323	0.12687	7.14413	6.87304	0.57968
TV-ℓ_2	25.1877	34.17228	0.12580	7.14413	6.78711	0.82976
NTV	24.6728	34.25736	0.12535	7.14413	6.65482	1.13269

Table 7: Statistical quality measurements for Salt & Pepper noise removal in images, noise ratio = 0.3, obtained results using TV-ℓ_1, TV-ℓ_2, and NTV models.

SQMs	MSE	PSNR	SSIM	Eo	Ed	Time (s)
TV-ℓ_1	38.73609	32.31198	0.08284	7.14413	6.66909	0.57587
TV-ℓ_2	37.28883	32.46829	0.08145	7.14413	6.51606	0.81025
NTV	36.99196	32.49846	0.08093	7.14413	6.25985	1.14645

Table 8: Statistical quality measurements for Salt & Pepper noise removal in images, noise ratio = 0.4, obtained results using TV-ℓ_1, TV-ℓ_2, and NTV models.

SQMs	MSE	PSNR	SSIM	Eo	Ed	Time (s)
TV-ℓ_1	50.54876	31.15618	0.05797	7.14413	6.42015	0.58367
TV-ℓ_2	49.42895	31.24427	0.05666	7.14413	6.21817	0.81161
NTV	49.26637	31.25439	0.05632	7.14413	5.80235	1.13793

Tables 5-8 showed the results using the NTV model outperformed those obtained using TV-ℓ_1, and TV-ℓ_2 in terms of noise removal and keeping edges for all these different noise ratios. Where, in the Salt & Pepper, Speckle, and Poisson noises, the MSE has a positive relationship with the noise ratios, where the value of MSE is increased when the value of noise ratios is increased, while the value of PSNR is increased when the noise ratios are decreased. While, in the Gaussian noise, MSE has an inverse relationship with the noise ratios because of the mechanism of adding Gaussian noise. Moreover, the above tables indicate that the NTV model is better at removing noise, it yields a higher PSNR with less MSE and gives an SSIM value closer to one. The NTV model also has an entropy close to the original image entropy than the TV-ℓ_1, and TV-$\ell_2$models.

4.3. Different iterations of numerical solutions

Statistical measurements are used in this experiment to examine the execution of the proposed model and the outcomes of these models at various iterations are compared with the TV-ℓ_1, and TV-ℓ_2 models. Those parabolic equations have a finite iteration number of numerical solutions to use for the removal of noise. The solutions of those models are examined at different iterations, and it is seen which model achieves a stable state very early and thus comes to the noise removal in images at a low iteration number. This experiment is conducted on 100 color images, the α and β are 0.001, and the Gaussian noise to images has been studied to check the performance of the proposed model at different iterations. Tables 9–12 summarize the average values of MSE, PSNR, SSIM, entropy, and the time taken to obtain results utilizing these models at different iterations.

Table 9: Statistical Quality measurements for Gaussian noise removal in images, iteration = 600, obtained results using TV-ℓ_1, TV-ℓ_2, and NTV models.

SQMs	MSE	PSNR	SSIM	Eo	Ed	Time (s)
TV-ℓ_1	57.04483	30.79851	0.52891	7.14413	6.82955	13.55861
TV-ℓ_2	49.07543	31.50311	0.56846	7.14413	6.91802	8.76532
NTV	41.15065	32.16501	0.68813	7.14413	7.13686	10.51648

Table 10: Statistical Quality measurements for Gaussian noise removal in images, iteration = 800, obtained results using TV-ℓ_1, TV-ℓ_2, and NTV models.

SQMs	MSE	PSNR	SSIM	Eo	Ed	Time (s)
TV-ℓ_1	60.46011	30.52612	0.51163	7.14413	6.79819	17.91182
TV-ℓ_2	49.60392	31.45191	0.56576	7.14413	6.90715	11.39328
NTV	36.93461	32.73582	0.73674	7.14413	7.05192	13.50584

Table 11: Statistical Quality measurements for Gaussian noise removal in images, iteration = 1000, obtained results using TV-ℓ_1, TV-ℓ_2, and NTV models.

SQMs	MSE	PSNR	SSIM	Eo	Ed	Time (s)
TV-ℓ_1	62.96939	30.33977	0.50031	7.14413	6.77245	29.26082
TV-ℓ_2	49.95006	31.41951	0.56405	7.14413	6.89734	13.77505
NTV	36.51081	32.85549	0.73667	7.14413	6.99208	19.51194

Table 12: Statistical Quality measurements for Gaussian noise removal in images, iteration = 1200, obtained results using TV-ℓ_1, TV-ℓ_2, and NTV models.

SQMs	MSE	PSNR	SSIM	Eo	Ed	Time (s)
TV-ℓ_1	65.14019	30.18467	0.49203	7.14413	6.75092	31.77059
TV-ℓ_2	50.33899	31.38188	0.56303	7.14413	6.89375	16.74161
NTV	37.68867	32.73836	0.71700	7.14413	6.94867	20.10283

Tables 9-12 showed the results using the NTV model outperformed those obtained using TV-ℓ_1, and TV-ℓ_2 in terms of noise removal and keeping edges for all these iterations. The

solutions of the NTV model take a higher number of iterations to arrive at a steady state rapidly than TV-ℓ_1, and TV-ℓ_2 models through removing noise from the image. Moreover, the values of MSE, PSNR, SSIM, and entropy using the NTV model are better than those obtained using the TV-ℓ_1, and TV-$\ell_2$models.

4.4. Different values of α and β parameters

In this experiment, the NTV model performance is studied using different values of α and β parameters and their effects on it. Firstly, different values of α and β parameters are studied in this experiment as seen in Table 13.

Table 13: Different values of $\alpha, and\ \beta$ parameters.

β value	α value
1	0.001
0.001	1
1.5	0.5
0.5	1.5

This experiment was conducted on 100 color images. The Gaussian noise to images has been used, the iteration was 1000, and the results of the NTV model are contrasted with those obtained using TV-ℓ_1, and TV-ℓ_2 models. Tables 14-17 summarize the average values of MSE, PSNR, SSIM, entropy, and the time taken to obtain results utilizing these models.

Table 14: Statistical Quality measurements for Gaussian noise removal in images, iteration =1000 obtained results using NTV models.

SQMs	MSE	PSNR	SSIM	Eo	Ed	Time (s)
$\alpha = 0.001, \beta = 1$	36.49688	32.85785	0.73653	7.14413	6.99210	17.75818
$\alpha = 1, \beta = 0.001$	42.73888	32.08741	0.72267	7.14413	7.10464	17.38383
$\alpha = 1.5, \beta = 0.5$	38.65261	32.55823	0.73838	7.14413	7.07381	17.33134
$\alpha = 0.5, \beta = 1.5$	46.48681	31.72723	0.69439	7.14413	7.04370	17.97016

The results of the proposed model were not promising, as seen in Table 14. The results weren't stable, and the model's performance wasn't good. Therefore, the α and β parameters are chosen at the same value and are applied in this experiment under the same conditions as seen in Table 15.

Table 15: The same values of $\alpha, and\ \beta$ parameters.

β value	α value
0.001	0.001
0.5	0.5
1	1
1.5	1.5

This experiment is conducted on 100 color images. The Gaussian noise to images has been used, the iteration was 1000, and the results of the NTV model are contrasted with those

obtained using TV-ℓ_1, and TV-ℓ_2 models. Tables 16–19 summarize the average values of MSE, PSNR, SSIM, entropy, and the time taken to obtain results utilizing these models.

Table 16: Statistical Quality measurements for Gaussian noise removal in images, $\alpha = 0.001, \beta = 0.001$, obtained results using TV-ℓ_1, TV-ℓ_2, and NTV models.

SQMs	MSE	PSNR	SSIM	Eo	Ed	Time (s)
TV-ℓ_1	62.96938	30.33976	7.14413	0.50031	6.77245	29.26081
TV-ℓ_2	49.95005	31.41951	7.14413	0.56405	6.89734	13.77505
NTV	36.51079	32.85549	7.14413	0.73667	6.99208	19.51193

Table 17: Statistical Quality measurements for Gaussian noise removal in images, $\alpha = 0.5, \beta = 0.5$, obtained results using TV-ℓ_1, TV-ℓ_2, and NTV models.

SQMs	MSE	PSNR	SSIM	Eo	Ed	Time (s)
TV-ℓ_1	63.60143	30.28420	7.14413	0.49819	6.71307	22.04809
TV-ℓ_2	80.13568	29.14319	7.14413	0.38034	7.46905	14.76103
NTV	42.70003	32.09748	7.14413	0.72428	7.06660	17.08428

Table 18: Statistical Quality measurements for Gaussian noise removal in images, $\alpha = 1, \beta = 1$, obtained results using TV-ℓ_1, TV-ℓ_2, and NTV models.

SQMs	MSE	PSNR	SSIM	Eo	Ed	Time (s)
TV-ℓ_1	63.04330	30.32704	7.14413	0.49798	6.73488	22.11825
TV-ℓ_2	82.04102	29.03929	7.14413	0.37040	7.45529	14.07832
NTV	46.30421	31.74700	7.14413	0.69541	7.04172	17.10227

Table 19: Statistical Quality measurements for Gaussian noise removal in images, $\alpha = 1.5, \beta = 1.5$, obtained results using TV-ℓ_1, TV-ℓ_2, and NTV models.

SQMs	MSE	PSNR	SSIM	Eo	Ed	Time (s)
TV-ℓ_1	62.62307	30.35748	7.14413	0.49800	6.75294	22.14567
TV-ℓ_2	82.54623	29.01225	7.14413	0.36723	7.44972	14.07469
NTV	46.41346	31.73357	7.14413	0.69454	7.04323	17.10031

Tables 16–19 showed the results using the NTV model outperformed those obtained using TV-ℓ_1, and TV-ℓ_2 in terms of noise removal and keeping edges for all these different values of α and β parameters. The best results of the proposed model were when the values of α and β parameters were 0.001. Moreover, the above tables indicate that the NTV model is better at removing noise, it yields a higher PSNR with less MSE and gives an SSIM value closer to one. The NTV model also has an entropy closer to the original image entropy than the TV-ℓ_1, and TV-$\ell_2$models.

5. Conclusion and Future Work

In this paper, a new image-denoising model was proposed based on combining TV-ℓ_1, and TV-ℓ_2. Then IFDM is used to find the numerical solutions for the proposed model. These

numerical results have been compared with those obtained using TV-$\ell_1$and TV-ℓ_2 models based on statistical metrics. Different numerical experiments have been conducted to study and check the efficacy and efficiency of the performance proposed model for noise removal in color images. The quality of denoised images is checked through comparison with original noise images, using MSE, PSNR, SSIM, and entropy, which is seen in these experiments as follows:

Firstly, the NTV model has been applied to remove different types of noise, such as Gaussian, Speckle, Poisson, and Salt & Pepper. It is shown that the numerical solutions of the NTV model are the best, and its performance surpasses that of other models for all these types of noise.

Secondly, evaluating the performance of the proposed model compared to other models using different Salt &Pepper noise ratios, which are 0.1, 0.2, 0.3, and 0.4, it is noticed that the model's performance is inversely proportional to the noise ratio. In comparison, maintaining its efficiency compared to other models based on all these SQMs. It is also observed that the model performance is proportional to the noise ratio when using the Gaussian noise type. This is due to adding noise to this type, which improves the model's performance when the noise percentage increases. From these results, it is noted that when there is a significant amount of noise in the data, the model can adapt to these conditions and maintain acceptable performance compared to other models.

In another experiment, the behavior of the proposed model was studied using different iterations through Gaussian noise removal. It was noticed that the proposed model needed a high number of iterations to reach a steady state, while other models required a few iterations. Fourthly, the efficiency of the proposed model is studied using different α and β values. In this experiment, two different procedures were conducted for choosing these parameters when the values of α and β are different through Gaussian noise removal in images. It was found that the proposed model has better efficiency than other models, but the results weren't stable. While the values of α and β are the same through Gaussian noise removal in images, it is found that the proposed model has better efficiency than other models, and its efficiency increases as the parameter values approach zero.

Finally, all these experiments have proven the results of the NTV model to overcome the results of other models. Also, the NTV model visually succeeded in removing the noise in the images in terms of preserving the texture (i.e. edges and corners) in the photos. This means the NTV model was applied to remove noise in images and performed well in preserving edges during noise removal. Furthermore, the connectivity principle is satisfied, and the curvature is maintained.

References

[1] T. F. Chan, J. Shen, and L. Vese, "Variational PDE Models in Image Processing," *Notices AMS*, vol. 50, no. 1, pp. 14-26, 2003.

[2] Bing Song, "*Topics in variational PDE image segmentation, inpainting, and denoising," University of California, Los Angeles*, 2003.

[3] A. de Cheveigné and J. Z. Simon, "Sensor noise suppression," *Journal of Neuroscience Methods*, vol. 168, no. 1, p. 195, Feb. 2008.

[4] A. Chambolle, R. A. Devore, N.-Y. Lee, and B. J. Lucier, "Nonlinear Wavelet Image Processing: Variational Problems, Compression, and Noise Removal through Wavelet Shrinkage," *IEEE Transaction on Image Processing*, vol. 7, no. 3, pp. 319-335, 1998.

[5] K. Joo and S. Kim, "PDE-based image restoration: A hybrid model and color image denoising," *IEEE Transaction on Image Processing*, vol. 15, no. 5, pp. 1163-1170, 2006.

[6] C. Dumitrescu, M. S. Raboaca, and R. A. Felseghi, "Methods for Improving Image Quality for Contour and Textures Analysis Using New Wavelet Methods," *Applied Sciences 2021,* vol. 11, no. 9, p. 3895, Apr. 2021.

[7] A. K. Al-Jaberi, E. M. Hameed, "A Review of PDE Based Local Inpainting Methods," *In Journal of Physics: Conference Series*, vol. 1818, no. 1, p. 012149, 2021.

[8] M. Bertalmío, Ed., *"Denoising of Photographic Images and Video: Fundamentals, open Challenges, and New Trends," Springer*, 2018, p. 333.

[9] H. Wang, L. Fan, Q. Guo, and C. Zhang, "A review of image denoising methods," *Communications in Information and Systems*, vol. 20, no. 4, pp. 461–480, 2020.

[10] I. Markovsky, *Low-Rank Approximation: algorithms, implementations, applications*, *Springer*, 2012.

[11] W. Dong, L. Zhang, G. Shi, and X. Li, "Nonlocally centralized sparse representation for image restoration," *IEEE Transactions on Image Processing*, vol. 22, no. 4, pp. 1620–1630, 2013.

[12] C. Tian, L. Fei, W. Zheng, Y. Xu, W. Zuo, and C.-W. Lin, "Deep Learning on Image Denoising: An Overview," *Neural Networks*, vol. 131, pp. 251-275, 2020.

[13] H. Wang, Y. Wang, and W. Ren, "Image denoising using anisotropic second and fourth order diffusions based on gradient vector convolution," *Computer Science and Information Systems*, vol. 9, no. 4, pp. 1493–1511, 2012.

[14] L. I. Rudin, S. Osher, and E. Fatemi, "Nonlinear total variation based noise removal algorithms," *Physica D*, vol. 60, no. 1–4, pp. 259–268, Nov. 1992.

[15] P. Blomgren, T. F. Chan, P. Mulet, and C. K. Wong, "Total Variation Image Restoration: Numerical Methods and Extensions," *In proceedings of international conference on image processing*, vol. 3, pp. 384–387, 1997.

[16] C. Poon, "On the Role of Total Variation in Compressed Sensing," *SLAM Journal on Imaging Sciences*, vol. 8, no. 1, pp. 682–720, Mar. 2015.

[17] D. Perrone, and P. Favaro, "Total variation blind deconvolution: The devil is in the details," *In Proceedings of the IEEE Conference on Computer Vision and Pattern Recognition*, Vancouver, 2014.

[18] S. Bartels, R. H. Nochetto, and A. J. Salgado, "A total variation diminishing interpolation operator and applications," *Mathematical of Computation*, vol. 84, no. 296, pp. 2569–2587, Mar. 2015.

[19] A. Al-Jabari, N. Al-Jawad, and S. A. Jassim, "Colourizing monochrome images," in *Mobile Multimedia/Image Processing, Security, and Applications 2018*, SPIE, vol. 10668, no.14, pp. 25-37, Orlando, May 2018.

[20] J. Bect, L. Blanc-Féraud, G. Aubert, and A. Chambolle, "A l 1-Unified Variational Framework for Image Restoration," *Lecture Notes in Computer Science (including subseries Lecture Notes in Artificial Intelligence and Lecture Notes in Bioinformatics)*, vol. 3024, pp. 1–13, 2004.

[21] Y. Hu and M. Jacob, "Higher degree total variation (HDTV) regularization for image recovery," *IEEE Transactions on Image Processing*, vol. 21, no. 5, pp. 2559–2571, May 2012.

[22] B. Yang, H. Xia, M. Annor-Nyarko, and Z. Wang, "Application of total variation denoising in nuclear power plant signal pre-processing," *Annals of Nuclear Energy*, vol. 135, p. 106981, Jan. 2020.

[23] M. V. Afonso and J. M. R. Sanches, "Blind Inpainting Using ℓ0 and Total Variation Regularization," *IEEE Transactions on Image Processing*, vol. 24, no. 7, pp. 2239–2253, Jul. 2015.

[24] M. Grasmair and F. Lenzen, "Anisotropic total variation filtering," *Applied Mathematics Optimization*, vol. 62, no. 3, pp. 323–339, Dec. 2010.

[25] Q. Chen, P. Montesinos, Q. Sen Sun, P. A. Heng, and D. S. Xia, "Adaptive total variation denoising based on difference curvature," *Image and Vision Computing*, vol. 28, no. 3, pp. 298–306, 2010.

[26] L. Guo, X. Le Zhao, X. M. Gu, Y. L. Zhao, Y. B. Zheng, and T. Z. Huang, "Three-dimensional fractional total variation regularized tensor optimized model for image deblurring," *Applied Mathematics Computation*, vol. 404, no. 1, p. 126224, Sep. 2021.

[27] C. T. Pham, T. Tran, H. V. Dang, and H. P. Dang, "An adaptive image restoration algorithm based on hybrid total variation regularization," *Turkish Journal of Electrical Engineering & Computer Sciences*, vol. 31, no. 1, pp. 1–17, 2023.

[28] P. Rodríguez, "Total variation regularization algorithms for images corrupted with different noise models: A review," *Journal of Electrical and Computer Engineering*, 2013.

[29] A. J. Harfash, "Numerical Methods for Solving Some Hydrodynamic Stability Problems," *International Journal Application Computation. Math*, vol. 1, pp. 293–326, 2015.

[30] Zainab J. Kadum and Noori Y. Abdul-Hassan, "New Numerical Methods for Solving the Initial Value Problem Based on a Symmetrical Quadrature Integration Formula Using Hybrid Functions," *MDPI*, vol. 15, no. 3, Feb. 2023.

[31] M. J. A.-K. A.S.J. and Al-Saif, "Alternating Direction Implicit Formulation of the Differential Quadrature Method for Solving Burger Equations," *International Journal of Modern Mathematical Sciences,* vol. 1, no. 3, pp. 1–11, 2012.

[32] P. Arbelaez, C. Fowlkes, and D. M. Pablo, "The Berkeley Segmentation Dataset and Benchmark," 2007. The website of the Berkeley database is available at: https://www2.eecs.berkeley.edu/Research/Projects/CS/vision/bsds/

[33] A. Popowicz, and B. Smolka, "Overview of Grayscale Image Colorization Techniques," *Color Image and Video Enhancement*, pp. 345–370, Jan. 2015.

[34] Z. Wang, A. C. Bovik, H. R. Sheikh, and E. P. Simoncelli, "Image quality assessment: From error visibility to structural similarity," *IEEE Transactions on Image Processing*, vol. 13, no. 4, pp. 600–612, Apr. 2004.

[35] D. Y. Tsai, Y. Lee, and E. Matsuyama, "Information entropy measure for evaluation of image quality," *Journal of Digitial Imaging*, vol. 21, no. 3, pp. 338–347, Sep. 2008.

[36] H. Y. Khaw, F. C. Soon, J. H. Chuah, and C. O. Chow, "Image noise types recognition using convolutional neural network with principal components analysis," *IET Image Processing*, vol. 11, no. 12, pp. 1238–1245, Dec. 2017.